

# Indirect nuclear exchange coupling and electronic structure of the chain semiconductor TlSe: A $^{203}\text{Tl}$ and $^{205}\text{Tl}$ NMR study

A. M. Panich<sup>1,\*</sup> and N. M. Gasanly<sup>2</sup><sup>1</sup>*Department of Physics, Ben-Gurion University of the Negev, P.O. Box 653, Beer-Sheva 84105, Israel*<sup>2</sup>*Department of Physics, Middle East Technical University, Ankara 06531, Turkey*

(Received 20 October 2000; published 9 April 2001)

We report an NMR study of the indirect nuclear exchange coupling, electronic structure, and wave-functions overlap in the single crystal of semiconductor TlSe which has a chain structure and comprises two kinds of Tl atoms,  $\text{Tl}^{1+}$  and  $\text{Tl}^{3+}$ . Strong exchange coupling among the spins of  $\text{Tl}^{1+}$  and  $\text{Tl}^{3+}$  ions, which reside in neighboring chains, is observed. This interaction is significantly stronger than the exchange coupling of the equivalent atoms within the chains. Such an interchain coupling is realized due to the overlap of the  $\text{Tl}^{1+}$  and  $\text{Tl}^{3+}$  electron wave functions across the intervening Se atom. The aforementioned wave-function overlap is the dominant mechanism in the formation the uppermost valence bands and lower conduction bands in TlSe and determines the electronic structure and the main properties of the compound.

DOI: 10.1103/PhysRevB.63.195201

PACS number(s): 71.20.Nr

## I. INTRODUCTION

Chain and layered  $\text{Tl(I)M(III)X}_2$  ( $M = \text{Tl, Ga, In, X} = \text{Se, S, Te}$ ) semiconductors are of great interest because of their low dimensionality, photoconductivity, and potential applications for optoacoustics and optoelectronics. Recent  $^{203}\text{Tl}$  and  $^{205}\text{Tl}$  nuclear magnetic resonance (NMR) studies of chain  $\text{TlGaTe}_2$  and layered  $\text{TlInS}_2$ ,  $\text{TlGaS}_2$ ,  $\text{TlGaSe}_2$ , and  $\text{Tl}_2\text{Te}_3$  semiconductors revealed strong indirect nuclear spin-exchange couplings between Tl isotopes, due to significant interchain (in  $\text{TlGaTe}_2$ ) or interlayer (in  $\text{TlMX}_2$  and  $\text{Tl}_2\text{Te}_3$ ) overlap of the thallium electron wave functions across the intervening X atom.<sup>1-3</sup> Such considerable overlap affects the physical properties of these compounds.<sup>4</sup> In this paper, we report the NMR study of the indirect nuclear spin-exchange coupling, electronic structure, and wave-function overlap in the semiconductor compound TlSe, which has a chain structure and comprises two kinds of Tl atoms, namely  $\text{Tl}^{1+}$  and  $\text{Tl}^{3+}$ . Single crystal of TlSe was used for the measurements. Strong exchange coupling among the spins of  $\text{Tl}^{1+}$  and  $\text{Tl}^{3+}$  ions, which reside in the neighboring chains, is observed. This interaction is significantly stronger than the exchange coupling of the nuclei of the equivalent atoms within the chains. Such an interchain coupling is realized due to the overlap of the  $\text{Tl}^{1+}$  and  $\text{Tl}^{3+}$  electron wave functions across the intervening Se atom. The aforementioned wave-function overlap is the dominant mechanism of the formation of the uppermost valence bands and lower conduction bands in TlSe and determines the electronic structure and the main properties of the compound.

## II. CRYSTAL STRUCTURE AND ELECTRICAL PROPERTIES OF TlSe

The crystal structure of TlSe belongs to the tetragonal symmetry, the space group is  $D_{4h}^{18}-14/mcm$ , and the lattice parameters are  $a = b = 8.02 \text{ \AA}$  and  $c = 6.79 \text{ \AA}$ ,  $Z = 4$ .<sup>5,6</sup> TlSe is a mixed-valence compound. Its formula should be more accurately written as  $\text{Tl}^{1+}\text{Tl}^{3+}\text{Se}_2^{4-}$ . The trivalent and univa-

alent thallium ions occupy two crystallographically inequivalent sites. The  $\text{Tl}^{3+}$  cations form covalent ( $sp^3$ ) Tl-Se bonds and are located at the centers of  $\text{Tl}^{3+}\text{Se}_4^{2-}$  tetrahedra, which are linked by common horizontal edges and form linear chains along the  $c$  axis. The  $\text{Tl}^{3+}$ -Se distance,  $2.67 \text{ \AA}$ , is close to the sum of the covalent radii of Tl ( $1.49 \text{ \AA}$ ) and Se ( $1.17 \text{ \AA}$ ), respectively, the Se-Tl-Se angle is  $115^\circ$ . Each univalent  $\text{Tl}^{1+}$  cation is surrounded by eight chalcogen atoms, which form slightly deformed Thomson cubes that are skewed by a small angle. Columns of Thomson cubes with common square faces are parallel to the  $c$  axis and alternate with the columns of the aforementioned  $\text{Tl}^{3+}\text{Se}_4^{2-}$  tetrahedra.  $\text{Tl}^{1+}$ -Se distances are  $3.43 \text{ \AA}$ , a little shorter than the sum of the ionic radii of  $\text{Tl}^{1+}$  ( $1.73 \text{ \AA}$  for coordination number 8) and  $\text{Se}^{2-}$  ( $1.84 \text{ \AA}$ ). The  $\text{Tl}^{1+}$ - $\text{Tl}^{1+}$ , and  $\text{Tl}^{3+}$ - $\text{Tl}^{3+}$  distances in the chains are  $3.49 \text{ \AA}$ ,<sup>6</sup> while the distances between these atoms in the (001) plane are  $5.67 \text{ \AA}$ . Each  $\text{Tl}^{1+}$  ion has four  $\text{Tl}^{3+}$  neighbors at  $4.01 \text{ \AA}$  in the  $a, b$  plane, and, in reverse, each  $\text{Tl}^{3+}$  ion has four  $\text{Tl}^{1+}$  neighbors at the same distance. Projection of the TlSe structure on the (001) plane is shown in Fig. 1.

Electrical transport study and optical measurements have shown that TlSe is a semiconductor with the energy gap measured by different authors as 0.6 to 1.0 eV at 300 K.<sup>7,8</sup> Sugaïke<sup>9</sup> measured the anisotropy of the electric conductivity

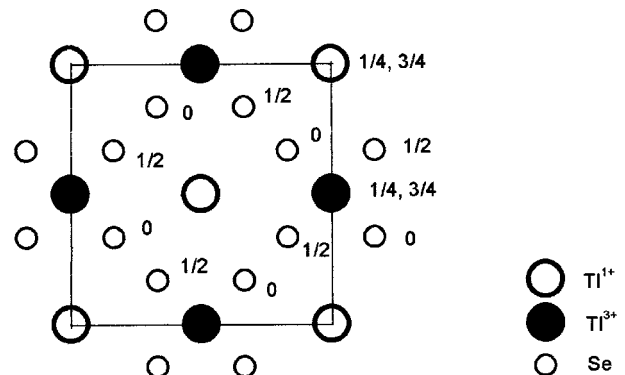


FIG. 1. Projection of the TlSe structure on the (001) plane.

of TlSe and reported that it is metallic in the (001) plane and semiconducting along the  $c$  axis. Abdullaev *et al.*,<sup>10</sup> who studied resistance and magnetoresistance of TlSe single crystals at 1.3 to 300 K, also observed a difference in resistivity in two directions, i.e., parallel and perpendicular to the  $c$  axis, in particular at low temperatures, from 1.3 to 5 K. However, this difference varied from sample to sample, showing both  $\rho_{\parallel} > \rho_{\perp}$  and  $\rho_{\parallel} < \rho_{\perp}$  cases. A “metallic” behavior, observed in some samples, was attributed to the impurity conductivity.

### III. EXPERIMENT

The single crystal of thallium selenide under study has a form of a parallelepiped of the size of  $12 \times 5 \times 2$  mm with its  $c$  axis along the longest edge of the parallelepiped; two other edges were along  $a$  and  $b$  axes.

Room-temperature  $^{203}\text{Tl}$  and  $^{205}\text{Tl}$  NMR measurements of the single crystal of TlSe were performed using a Tecmag pulse NMR spectrometer. The main experiments were carried out in the external magnetic fields  $B_0 = 1.23$  and  $8.0196$  T (the corresponding resonance frequencies of  $^{205}\text{Tl}$  isotope are 30.3 and 197.4 MHz), using a Varian electromagnet and an Oxford superconducting magnet, respectively. Some additional measurements were made in  $B_0 = 0.445, 0.62, 0.785,$  and  $1.015$  T, corresponding to the  $^{205}\text{Tl}$  resonance frequencies of 10.93, 15.23, 19.29, and 24.94 MHz, respectively. The Hahn echo,  $\pi/2 - \tau - \pi$  pulse sequence with phase cycling was used with a repetition time of  $5 T_1$ . At low-magnetic field the  $\pi/2$  pulse length was  $3.1 \mu\text{s}$ , while at high field, the  $\pi/2$  pulse length was  $3.7 \mu\text{s}$  for a cylindrical coil and  $5.5 \mu\text{s}$  for a saddle coil.

In high-magnetic field, thallium NMR spectra cover a range of several hundred kHz and cannot be excited by a single  $\pi/2$  pulse. Thus, the frequency was swept in steps ranging from 7 to 15 kHz, and the amplitude of the resulting Hahn echo was plotted versus the frequency. For comparison, the maxima of the Fourier transform of the Hahn echoes showed the same line shape. In the low-field case, the whole spectrum was obtained from the Fourier transform of the Hahn echo. The number of scans usually extended from 2048 to 5600 for  $^{205}\text{Tl}$  and from 48 000 to 160 000 for  $^{203}\text{Tl}$  in low-magnetic fields, while in  $8.0196$  T the number of scans was from 480 to 4096 for  $^{205}\text{Tl}$  and from 2048 to 20 480 for  $^{203}\text{Tl}$ , respectively.

To study the angular dependence of the NMR spectra in low-magnetic field, the single crystal was placed into a cylindrical coil and rotated around the vertical direction, achieving all  $(B_0, c)$  angles between  $0$  and  $90^\circ$ . In high-magnetic field, we used both a common cylindrical coil oriented perpendicular to the applied magnetic-field  $B_0$  (to measure the spectrum for  $B_0 \perp c$ ), and the saddle coil (of the size of the crystal) that was tilted at different angles with respect to  $B_0$ , holding the radio frequency field  $B_1 \perp B_0$ .

Thallium NMR shifts are given relative to an aqueous  $0.002 \text{ mol dm}^{-3}$  solution of  $\text{TlNO}_3$ , the position of which is assigned to the value of  $0 \text{ ppm}$ .<sup>11</sup> In our measurements, we used a  $0.3 \text{ mol dm}^{-3}$  aqueous solution of  $\text{Tl}(\text{NO}_3)_3$  and  $\text{TlCl}$  powder [ $\delta = +383 \text{ ppm}$  (Ref. 11)] as secondary references.

The cubic symmetry of the Tl site in  $\text{TlCl}$  yields a rather narrow line ( $\Delta\nu \sim 5 \text{ kHz}$ ), which is easily detectable. In our measurements, the aqueous solution of  $\text{Tl}(\text{NO}_3)_3$  showed the  $^{205}\text{Tl}$  resonance at  $196.9360 \text{ MHz}$  in  $B_0 = 8.0196 \text{ T}$ , and the position of the  $^{205}\text{Tl}$  signal of powder  $\text{TlCl}$  was at  $197.010153 \text{ MHz}$ .

### IV. INDIRECT NUCLEAR EXCHANGE IN SOLIDS—THEORETICAL BACKGROUND

Indirect coupling of two neighbor nuclei is realized across their overlapping electron clouds. This coupling,  $J_{12}\mathbf{I}_1\mathbf{I}_2$ , is bilinear in two nuclear-spin moments, and its size can be estimated from second-order perturbation theory. Van Vleck has shown<sup>12</sup> that like and unlike spins yield different contribution to the second moment of the NMR line,

$$S_2 = \int_0^\infty \nu^2 f(\nu) d\nu / \int_0^\infty f(\nu) d\nu, \quad (1)$$

where the numerator can be represented as

$$\begin{aligned} \int_0^\infty \nu^2 f(\nu) d\nu &= \frac{1}{2} \int_{-\infty}^{+\infty} \sum_{a,b} \nu^2 (a|I_x|b)(b|I_x|a) \\ &\quad \times \delta(E_a - E_b - \hbar\nu) d\nu \\ &= \frac{1}{2\hbar^3} \text{Tr}\{[H, I_x]^2\}, \end{aligned} \quad (2)$$

where  $f(\nu)$  is the line shape and  $H$  is the spin Hamiltonian of the system. For identical nuclei, the exchange term  $J_{12}\mathbf{I}_1\mathbf{I}_2$  commutes with  $I_x = I_{1x} + I_{2x}$ , and therefore has no effect on the second moment but does increase the fourth moment, giving rise to exchange narrowing of the central part of the resonance line. If the two nuclei are not identical, one can approximate the exchange coupling as  $J_{12}I_{1z}I_{2z}$ , which does not commute with  $I_x = I_{1x} + I_{2x}$  and, therefore, increases the second moment. Thus, in the crystal that contains two different types of atoms (or isotopes) having spins  $I$  and  $I'$ , the exchange contribution to the second moment of the unprimed spins, which are assumed to be responsible for the resonance absorption at the wave length being utilized, is given by

$$S_2 = \frac{1}{3} I'(I'+1) \sum_{k'} J_{jk'}^2, \quad (3)$$

with the sum on the primed spins only. Therefore,  $S_2$  is proportional to the abundance of the primed isotopes. The consequence of the Van Vleck's theory is that the ratio of the second moments of two different isotopes is inversely proportional to the ratio of their natural abundances. For thallium, the natural abundances are  $f = 29.5\%$  for  $^{203}\text{Tl}$  and  $(1-f) = 70.5\%$  for  $^{205}\text{Tl}$ , which makes the aforementioned effect readily observable. The first experimental evidence of such an effect (in  $\text{Tl}_2\text{O}_3$ ) was reported in the classic paper of Bloembergen and Rowland;<sup>13</sup> then it was observed by the other authors (e.g., Refs. 14, 15).

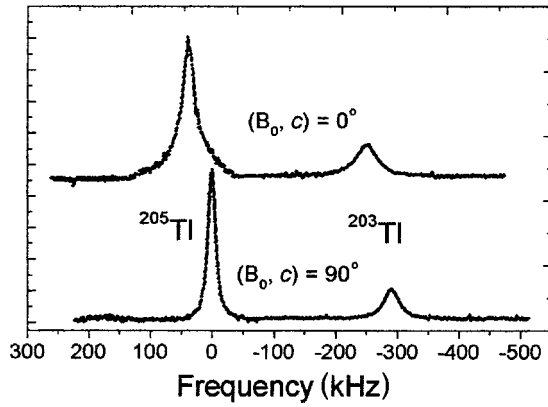


FIG. 2. Room temperature  $^{203}\text{Tl}$  and  $^{205}\text{Tl}$  NMR spectra at resonance frequency 30.3 MHz and  $B_0 \parallel c$  (top) and  $B_0 \perp c$  (bottom).

For TlSe, the aforementioned exchange coupling among  $^{205}\text{Tl}$  and  $^{205}\text{Tl}$  isotopes is expected for structurally equivalent Tl atoms in chains. Nuclear exchange of the  $^{205}\text{Tl}$ - $^{205}\text{Tl}$  and  $^{203}\text{Tl}$ - $^{203}\text{Tl}$  types would lead to the exchange narrowing of the corresponding resonances, while the  $^{203}\text{Tl}$ - $^{205}\text{Tl}$  exchange coupling would yield the second moment increase (i.e., broadening) of both  $^{203}\text{Tl}$  and  $^{205}\text{Tl}$  resonances. Besides this effect, we also expected to observe nuclear exchange interaction between the spins of Tl isotopes of structurally inequivalent  $\text{Tl}^{1+}$  and  $\text{Tl}^{3+}$  ions, which reside in neighboring chains. We hoped to resolve the resonances of these ions by means of measurement of a single-crystal sample in high-magnetic field, when the difference in chemical shifts of each isotope, belonging to the  $\text{Tl}^{1+}$  and  $\text{Tl}^{3+}$  ions, would exceed the exchange coupling between them. In such a case, all nuclei are unlike ones, and line broadening is expected not only for  $^{203}\text{Tl}$ - $^{205}\text{Tl}$  but also for  $^{205}\text{Tl}$ - $^{205}\text{Tl}$  and  $^{203}\text{Tl}$ - $^{203}\text{Tl}$  exchange interactions.

## V. RESULTS

Room-temperature thallium spectra of the single-crystal TlSe at frequency 30.3 MHz for  $B_0 \parallel c$  and  $B_0 \perp c$  are given in Fig. 2. For  $B_0 \perp c$ , both  $^{203}\text{Tl}$  and  $^{205}\text{Tl}$  isotopes show single-symmetric Lorentzian-like resonances with the second moments  $S_2 = 150 \pm 7$  and  $360 \pm 16 \text{ kHz}^2$  for  $^{205}\text{Tl}$  and  $^{203}\text{Tl}$ , respectively. The values of  $S_2$  are more than two orders of magnitude larger than the contributions of the dipole-dipole interactions of nuclear spins, estimated from the structure of TlSe as  $S_{2dd} \sim 1 \text{ kHz}^2$ . It means that another mechanism determines the line shape. The essential difference in the second moments of two thallium isotopes, together with the Lorentzian line shape, readily indicates that the strong exchange interaction between  $^{203}\text{Tl}$  and  $^{205}\text{Tl}$  nuclei is dominant.<sup>12,13</sup> The ratio of the second moments of two different Tl isotopes for  $B_0 \perp c$  was found to be  $S_2(\text{Tl}^{203})/S_2(\text{Tl}^{205}) = 2.4$ . This value is close to the reciprocal ratio of their natural abundances  $(1-f)(\text{Tl}^{205})/f(\text{Tl}^{203}) = 2.39$ , showing the value characteristic for the exchange coupling among Tl nuclei. Moreover, instead of two lines for each isotope expected for the two structurally inequivalent sites occupied by the trivalent and univalent thallium ions,<sup>5,6</sup>

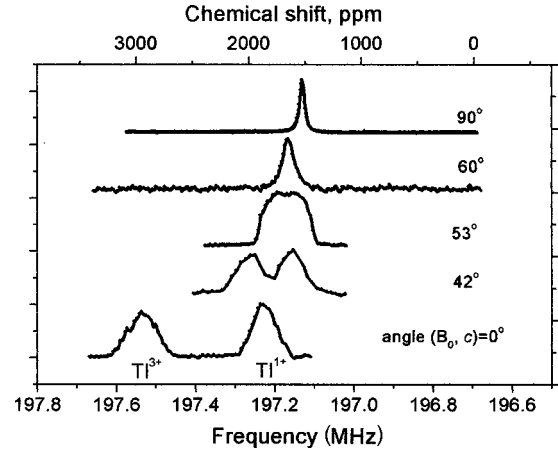


FIG. 3. Angular dependence of room temperature  $^{205}\text{Tl}$  NMR spectra at resonance frequency 197.4 MHz.

the single  $^{203}\text{Tl}$  and  $^{205}\text{Tl}$  resonances were obtained in all orientations of  $B_0$  with respect to the  $c$  axis at resonant frequencies up to 30.3 MHz (Fig. 2). This fact allows us to suggest a strong exchange interaction between nuclei of  $\text{Tl}^{1+}$  and  $\text{Tl}^{3+}$  ions that leads to a collapse of their resonances.

This assumption is readily supported by the high-field NMR measurements. Room-temperature  $^{205}\text{Tl}$  NMR spectra of the single crystal TlSe at frequency 197.4 MHz are given in Fig. 3. At  $B_0 \parallel c$ , the  $^{205}\text{Tl}$  spectrum shows two separate lines attributed to the  $\text{Tl}^{1+}$  and  $\text{Tl}^{3+}$  ions. When the applied magnetic field  $B_0$  is tilted from the  $c$  axis, two lines move to each other and finally collapse at  $\theta(B_0, c) \sim 55^\circ$ . Such a behavior is characteristic for the exchange interaction between the nuclei at inequivalent sites. Thus, we conclude that besides the common intrachain Tl-Tl exchange interaction, the exchange coupling between nuclei of structurally inequivalent  $\text{Tl}^{1+}$  and  $\text{Tl}^{3+}$  ions, which reside in neighboring chains, is realized in TlSe. We note that the  $^{205}\text{Tl}$  linewidth at  $B_0 \parallel c$  is larger than that at  $B_0 \perp c$  (Fig. 3) by a factor of 2.5. This is due to an additional broadening caused by the interchain exchange coupling, which likely dominates over the intrachain one.

The tetragonal symmetry of the thallium sites<sup>5,6</sup> should correspond to an axially symmetric chemical shielding tensor,

$$\sigma = \sigma_i + [(\sigma_{\parallel} - \sigma_{\perp})/3] \times (3 \cos^2 \theta - 1). \quad (4)$$

Here,  $\sigma_i$  is the isotropic part of the chemical shift,  $\sigma_{\parallel}$  and  $\sigma_{\perp}$  are parallel and perpendicular components of the shielding tensor, and  $\theta$  is the angle between the applied magnetic field  $B_0$  and the  $c$  axis. As seen in Fig. 3, when  $B_0$  is applied along the  $c$  axis, the  $^{205}\text{Tl}$  spectrum shows two lines at 197.2215 and 197.5152 MHz, corresponding to the chemical shifts of 1457 and 2950 ppm relative to the liquid  $\text{TlNO}_3$ . The chemical shift of the low-frequency line is close to the value of  $\sigma_{\parallel} = 1780$  ppm of  $\text{Tl}^{1+}$  ion in the isostructural compound  $\text{TlGaTe}_2$  (whose formula is written as  $\text{Tl}^{1+}\text{Ga}^{3+}\text{Te}_2^{4-}$ ) (Ref. 1) (Fig. 3). Thus, this line is attributed to the signal of  $^{205}\text{Tl}^{1+}$  ions in TlSe, with  $\sigma_{\parallel}(\text{Tl}^{1+}) = 1457$  ppm. The position of the high-frequency resonance is typical for  $\text{Tl}^{3+}$  [for in-

stance, solid  $\text{TlCl}_3$  shows  $\sigma = +2458$  ppm (Ref. 11)] and, thus, this line was attributed to the signal of  $^{205}\text{Tl}^{3+}$  ions, with  $\sigma_{\parallel}(\text{Tl}^{3+}) = 2950$  ppm. Because of the collapse of  $\text{Tl}^{1+}$  and  $\text{Tl}^{3+}$  lines at  $B_0 \perp c$ , the perpendicular components of the shielding tensors of nuclei of  $\text{Tl}^{1+}$  and  $\text{Tl}^{3+}$  ions,  $\sigma_{\perp}$ , cannot be determined. We note, however, that for  $B_0 \perp c$  the line-width is practically field independent ( $\Delta\nu = 13.1$  and  $13.4$  kHz in magnetic fields of  $1.23$  and  $8.0196$  T, respectively), showing that the values of  $\sigma_{\perp}(\text{Tl}^{1+})$  and  $\sigma_{\perp}(\text{Tl}^{3+})$  are close to each other. Thus, they were both taken at the resonance position for  $B_0 \perp c$  at  $197.1297$  MHz, as  $\sigma_{\perp} = 990$  ppm. We note that the value of  $\sigma_{\perp}(\text{Tl}^{1+})$  in the isostructural  $\text{TlGaTe}_2$  is  $1264$  ppm.<sup>1</sup> From the above data, one can find the isotropic parts of the chemical shifts  $\sigma_i(\text{Tl}^{1+}) = 1145$  ppm and  $\sigma_i(\text{Tl}^{3+}) = 1640$  ppm, corresponding to the frequencies of  $197.160$  and  $197.258$  MHz, respectively.

If we neglect a small contribution of the dipole-dipole and pseudo-dipole interactions, the Hamiltonian of the system under study will include Zeeman and scalar exchange terms and will be given as

$$\begin{aligned} \hat{H} = & -\gamma_{205}hB_0 \left( \sum_i I_{zi}^I + \sum_j I_{zj}^{III} \right) \\ & -\gamma_{203}hB_0 \left( \sum_{i'} I_{zi'}^I + \sum_{j'} I_{zj'}^{III} \right) + J_{11} \sum_{i,j} I_i^I I_j^I \\ & + J_{33} \sum_{i,j} I_i^{III} I_j^{III} + J_{13} \sum_{i,j} I_i^I I_j^{III}. \end{aligned} \quad (5)$$

Here,  $\gamma_{203}$  and  $\gamma_{205}$  are gyromagnetic ratios of  $^{203}\text{Tl}$  and  $^{205}\text{Tl}$  isotopes,  $J_{11}$  and  $J_{33}$  are the  $\text{Tl}^{1+} - \text{Tl}^{1+}$  and  $\text{Tl}^{3+} - \text{Tl}^{3+}$  exchange coupling constants in the chains along  $c$  axis, respectively, and  $J_{13}$  is the  $\text{Tl}^{1+} - \text{Tl}^{3+}$  exchange interaction between the chains, in the  $a, b$  plane. Spins  $I^I$  and  $I^{III}$  belong to the  $\text{Tl}^{1+}$  and  $\text{Tl}^{3+}$  (sites I and III) respectively;  $h$  is the Planck's constant. As is well known, NMR spectra of exchange coupled nuclei strongly depend on the ratio of the exchange constant  $J$  and NMR frequency difference of two species  $\delta$ .<sup>16-20</sup> Thus, the Hamiltonian Eq. (5) may be rewritten as

$$\begin{aligned} \hat{H} = & -\nu_{205}h \left( \sum_i I_{zi}^I + \sum_j I_{zj}^{III} \right) - \nu_{203}h \left( \sum_{i'} I_{zi'}^I + \sum_{j'} I_{zj'}^{III} \right) \\ & + \delta \times h \left( \sum_i I_{zi}^I - \sum_j I_{zj}^{III} \right) + \delta \times h \left( \sum_{i'} I_{zi'}^I - \sum_{j'} I_{zj'}^{III} \right) \\ & + J_{11} \sum_{i,j} I_i^I I_j^I + J_{33} \sum_{i,j} I_i^{III} I_j^{III} + J_{13} \sum_{i,j} I_i^I I_j^{III}, \end{aligned} \quad (6)$$

where  $\nu_{203}$  and  $\nu_{205}$  are the  $^{203}\text{Tl}$  and  $^{205}\text{Tl}$  NMR frequencies averaged over the sites I and III,  $\delta$  is the NMR frequency separation between sites I and III, and  $\nu = \gamma B_0$ . In the case in question, the separation  $\delta$  is driven by the angular dependence of the  $\text{Tl}^{1+}$  and  $\text{Tl}^{3+}$  chemical shifts given by

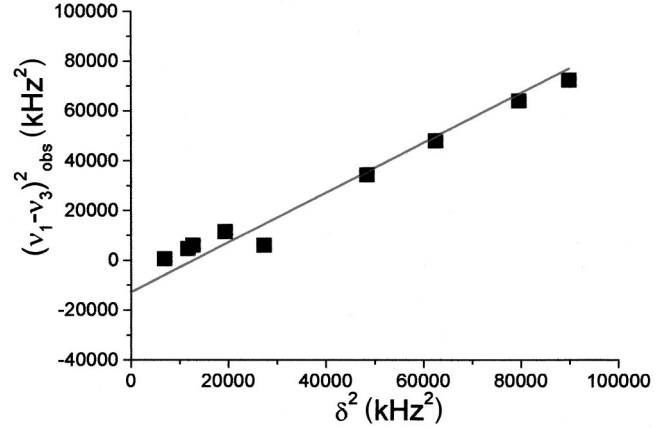


FIG. 4. Dependence of the experimentally observed squared separation between two peaks  $(\nu_1 - \nu_3)_{\text{obs}}^2$  of  $^{205}\text{Tl}$  NMR spectra ( $\nu_0 = 197.4$  MHz) on the squared separation without exchange  $\delta$  calculated from Eq. (7).

$$\begin{aligned} \delta = & (\sigma_{i3} - \sigma_{i1}) + \{[(\sigma_{3\parallel} - \sigma_{3\perp}) - (\sigma_{1\parallel} - \sigma_{1\perp})]/3\} \\ & \times (3 \cos^2 \theta - 1), \end{aligned} \quad (7)$$

where  $\sigma_1$  and  $\sigma_3$  belong to the  $\text{Tl}^{1+}$  and  $\text{Tl}^{3+}$ , respectively.

All experimental spectra may be analyzed in terms of the theory of the effect of exchange processes on NMR spectra.<sup>16-20</sup> Usually, this theory is applied for the study of chemical exchange, when a random jumping of the frequency from one value to another is realized due to a jump of a nucleus between two inequivalent sites belonging to one or the other of two molecules. In our case, the ‘‘motion’’ of spins is produced by spin-spin exchange interaction. The high-field spectra (Fig. 3) show that for the large angles  $\theta$  from  $60^\circ$  to  $90^\circ$ , the case of  $\delta < J_{13}$  is realized, while for the small angles,  $0^\circ < \theta < 55^\circ$ , we have  $\delta > J_{13}$ . The value of the ‘‘collapse angle’’ corresponds to  $\delta/J_{13} = 2\sqrt{2}$ ,<sup>17,18,20</sup> and thus, using Eq. (7) and the values of chemical shifts given above, one can estimate the value of the  $\text{Tl}^{1+} - \text{Tl}^{3+}$  exchange interaction as  $J_{13} \sim 38$  kHz.

In the case of the ‘‘intermediate’’ exchange rate,  $J_{13}$  can be found from the comparison of the separation between two maxima with the separation under conditions of slow exchange. The experimentally observed separation between two peaks  $(\nu_1 - \nu_3)_{\text{obs}}$  in this case is<sup>16-20</sup>

$$(\nu_1 - \nu_3)_{\text{obs}} = [\delta^2 - 8J_{13}^2]^{1/2}, \quad (8)$$

where  $\delta$  corresponds to the line separation calculated from Eq. (7) for  $\theta = 0$ . Figure 4 shows that the dependence of the squared peak separations of the high-field spectra  $(\nu_1 - \nu_3)_{\text{obs}}^2$  on  $\delta^2$  is linear, in agreement with Eq. (8). The analysis of this dependence using Eq. (8) yields  $J_{13} = 40.2 \pm 6$  kHz.

In the case of ‘‘slow exchange,’’ the value of  $J$  is relatively small in comparison to  $\delta$ , so that the principal effect is a broadening of the individual signals. This case is realized in the high-field spectra at  $B_0 \parallel c$  (Fig. 3). From Eq. (3) the  $^{205}\text{Tl}$  second moments in the position I and III are

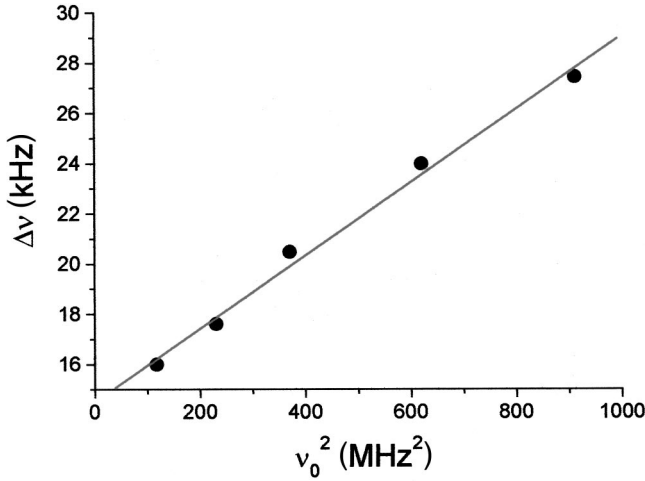


FIG. 5. Dependence of the  $^{205}\text{Tl}$  NMR line width on the resonance frequency for  $B_0\parallel c$ .

$$S_2(\text{I}) = J_{13}^2 + (f/2) \times J_{11}^2,$$

$$S_2(\text{III}) = J_{13}^2 + (f/2) \times J_{33}^2, \quad (9)$$

and should be close to each other if we assume that  $J_{11} \sim J_{33}$ . In this case, the exchange interaction of  $\text{TI}^{1+}$  and  $\text{TI}^{3+}$  spins is dominant, and therefore, the exchange narrowing of the resonance line is absent (see Sec. IV). If we neglect the contribution of intrachain exchange assuming that  $J_{13} \gg J_{11}$  and  $J_{13} \gg J_{33}$  (as mentioned above), the line profiles should be nearly Gaussian with the same line widths<sup>16–20</sup>

$$\Delta\nu = 2J_{13}. \quad (10)$$

Experiment shows that for  $B_0\parallel c$ , the  $\text{TI}^{1+}$  and  $\text{TI}^{3+}$  lines are almost Gaussian and their full line widths at half maximum height are close to each other,  $\Delta\nu(\text{TI}^{1+}) = 72$  kHz and  $\Delta\nu(\text{TI}^{3+}) = 84$  kHz, yielding  $J_{13} = 39 \pm 3$  kHz, in good agreement with the values of  $J_{13}$  found above. Slight difference in the linewidths may be assigned to a contribution of the intrachain exchange coupling, which is larger for  $\text{TI}^{1+}$  because of the presence of  $6s^2$ -electron pair (see discussion in the next section) and, thus, yields some exchange narrowing.

For  $\delta = 0$ , only exchange interactions with nuclei of unlike  $^{203}\text{Tl}$  and  $^{205}\text{Tl}$  isotopes contribute to the second moment of NMR spectra. Since  $\sigma_{\perp}(\text{TI}^{1+}) \approx \sigma_{\perp}(\text{TI}^{3+})$ , such a case is realized at  $B_0 \perp c$ . Experiment shows Lorentzian line shape (due to exchange narrowing<sup>16</sup>) with the full line width at half maximum height  $\Delta\nu_0 = 13$  kHz, which, as noted above, is nearly independent of  $B_0$ . The effective exchange constant in this case is

$$J_0 = (2J_{11}^2 + 2J_{33}^2 + 4J_{13}^2)^{1/2}. \quad (11)$$

It may be determined using Eq. (3) from the values of  $S_2(^{205}\text{Tl}) = 150$  kHz and  $S_2(^{203}\text{Tl}) = 360$  kHz at  $B_0 \perp c$ , which yield the value of  $J_0 = 45.1$  kHz.

For small  $J/\delta$  ratios (“fast exchange”), when two lines are collapsed, the additional line broadening is caused by the exchange interaction of spins in position I and III. As shown in references,<sup>17–20</sup> if we neglect a small contribution of

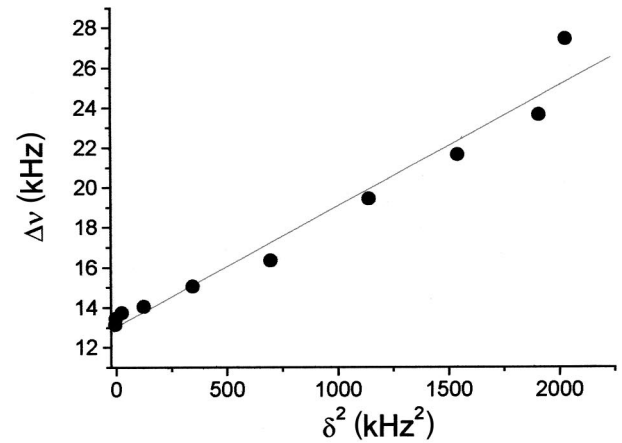
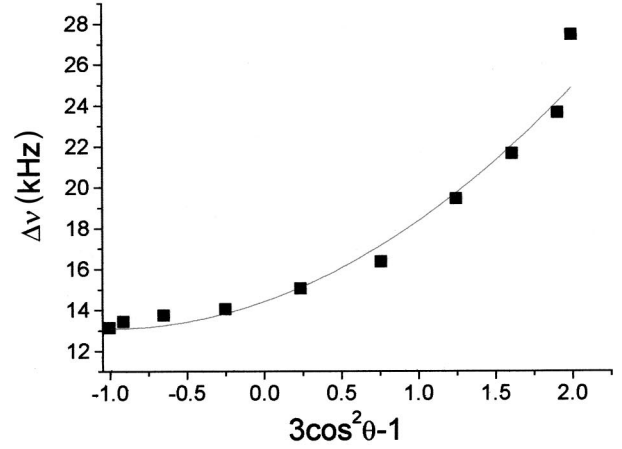


FIG. 6. Orientational dependence of the  $^{205}\text{Tl}$  NMR line width  $\Delta\nu$  at 30.3 MHz (top) and dependence of  $\Delta\nu$  on the square splitting  $\delta$  between  $\text{TI}^{1+}$  and  $\text{TI}^{3+}$  resonances calculated using Eq. (7) (bottom).

dipole-dipole interaction to the linewidth, this broadening is proportional to  $\delta^2$ , and since the populations of the sites I and III are equal ( $p_I = p_{\text{III}} = 1/2$ ), the linewidth may be given as

$$\Delta\nu = \Delta\nu_0 + \delta^2\nu^2/(4J_{13}). \quad (12)$$

(We use here the field independent value of  $\delta$  in units of ppm, thus, the spacing between signals in frequency units is  $\delta \times \nu$ ). Such a behavior is readily observed in the experiment. One can see from Fig. 5, that the dependence of  $\Delta\nu$  on the resonance frequency, measured for  $B_0\parallel c$  in the fields from 0.445 to 1.015 T (where the splitting between  $\text{TI}^{1+}$  and  $\text{TI}^{3+}$  peaks is still not observed) is practically linear in  $\nu^2$ . From this dependence, we found  $\Delta\nu_0 = 14.0 \pm 0.6$  kHz and  $\delta^2/4J_{13} = 14\,600 \pm 800$  kHz<sup>-1</sup>. The value of  $\delta = (\sigma_{3\parallel} - \sigma_{1\parallel}) = 1500$  ppm is known from the chemical shielding measurements. Analysis of this dependence yields  $J_{13} = 38.5 \pm 2$  kHz. Moreover, using Eqs. (7) and (12), the corresponding value of  $J_{13}$  may be found from the angular dependence of  $\Delta\nu$  in low-magnetic field, as shown in Fig. 6. The spectra at 30.3 MHz still does not show a splitting at  $B_0\parallel c$ , indicat-

ing that  $\delta < J$ . The dependence of  $\Delta\nu$  on  $\delta^2$  is linear and yields  $\Delta\nu_0 = 13.0 \pm 0.4$  kHz and  $J_{13} = 41.4 \pm 3$  kHz.

One can see that the values of  $J_{13}$  determined by different ways, are consistent with one another, showing the correctness of the aforementioned model of nuclear exchange. The average value of  $J_{13}$  is  $39.4 \pm 2.8$  kHz. Comparing this value with  $J_0 = (2J_{11}^2 + 2J_{33}^2 + 4J_{13}^2)^{1/2} = 45.1$  kHz, and assuming that  $J_1$  and  $J_{33}$  are equal, one can calculate the intrachain exchange constants  $J_{11} = J_{33} = 21.9$  kHz, which is only one-half the value of  $J_{13}$ .

## VI. DISCUSSION

As shown above, the exchange coupling among the spins of  $\text{Tl}^{1+}$  and  $\text{Tl}^{3+}$  ions, which belong to the neighboring chains, is significantly stronger than the exchange coupling of the equivalent atoms within the chains, though the distances between the equivalent Tl atoms in the chains (3.49 Å) are shorter than the  $\text{Tl}^{1+}-\text{Tl}^{3+}$  distances in the (001) plane (4.01 Å).<sup>5,6</sup> Since the  $\text{Tl}^{1+}-\text{Tl}^{3+}$  distance exceeds the sum of the ionic radii of  $\text{Tl}^{1+}$  and  $\text{Tl}^{3+}$ , the interchain exchange is evidently controlled by overlap of the  $\text{Tl}^{1+}$  and  $\text{Tl}^{3+}$  electron wave functions of the  $\text{Tl}^{1+}-\text{Se}-\text{Tl}^{3+}$  type across the intervening Se atoms. This overlap exceeds the corresponding overlap within the chains.

The band structure of the semiconductor under study would yield a long-range indirect nuclear exchange coupling. Common wave functions of Tl and Se guarantee, via electron-nuclear hyperfine interaction, an effective correlation of Tl nuclear spins. Indirect exchange coupling of the nuclear spins of atoms *A* and *B* can be expressed as a product of their hyperfine interaction constants  $J_A$  and  $J_B$  and squared overlap integral of the electron shells *S*:<sup>16,21</sup>

$$J_{AB} = J_A \times J_B S^2 / \Delta E. \quad (13)$$

Here,  $\Delta E$  is the energy gap between the conduction and the valence bands, averaged over the Brillouin zone. The electron configuration of the univalent thallium ion is  $5d^{10}6s^2$ , while the trivalent thallium ion shows the electron configuration  $5d^{10}$ . Since the contact hyperfine interaction,  $(8\pi/3)\gamma_n\gamma_e h^2 |\Psi(0)|^2$ , is realized by means of *s* parts of wave functions, which have a finite value  $|\Psi(0)|^2$  at the nucleus site,<sup>13</sup> an assistance of Tl  $6s^2$  electron pair is necessary.

The aforementioned exchange occurs via an intervening chalcogen atom, by analogy with the Kramers mechanism of electron-spin exchange via a nonmagnetic bridge ion.<sup>22</sup> As shown by Bloembergen and Rowland, this nuclear interaction is a kind of superexchange via intermediate excited electronic states.<sup>13</sup> Thus, to describe the indirect nuclear exchange interaction via a bridge atom, we should discuss the excited electronic states of  $\text{Tl}^{1+}$  and  $\text{Tl}^{3+}$  mixed with the states of the bridge  $\text{Se}^{2-}$  ion. For  $\text{Tl}^{1+}$  in TlSe, such interaction may be realized by means of mixing of Tl  $6s^2$  electron states with unoccupied  $4p$  states of Se. The Tl(I) orbitals are likely *sp*-hybridized Tl wave functions, which increases the

orbital overlap, since Tl*p* orbitals span a large range. Such a mixing of the  $\text{Tl}^{1+}$   $6p$  orbital into the filled Tl  $6s$  level was predicted by Orgel.<sup>23</sup>

One can suggest that a delocalized  $\text{Tl}^{1+}$   $6s^2$  electron pair could be shared among the univalent and trivalent Tl cations to guarantee the exchange coupling of  $\text{Tl}^{3+}$  ion. Though formally the  $\text{Tl}^{3+}$  ion has a configuration  $5d^{10}$ , covalent  $\text{Tl}^{3+}-\text{Se}^{2-}$  bonds with  $sp^3$  hybridization are suggested, since the  $\text{Tl}^{3+}-\text{Se}$  distance in tetrahedra is close to the sum of the covalent radii of Tl and Se. The presence of some portion of the *s* electron at the  $\text{Tl}^{3+}$  atom yields the electron-nuclear hyperfine interaction and explains the indirect exchange coupling of its spin.

We can conclude that  $\text{Tl}^{1+}-\text{Se}-\text{Tl}^{3+}$  overlap would be reflected in the formation of the valence and conduction bands. Thus, the Tl atoms play an important role in the establishment of semiconducting properties of TlSe.

Chemical shielding data readily support the aforementioned conclusions. As shown above, both univalent and trivalent Tl ions show essential chemical shielding anisotropy (CSA). For the spherically symmetric  $5d^{10}6s^2$  and  $5d^{10}$  electron configurations of the  $\text{Tl}^{1+}$  and  $\text{Tl}^{3+}$  ions, respectively, the shielding anisotropy is absent. Thus, one is led to consider *sp* hybridization of the Tl wave functions, which interact with the Se *p* orbitals and yield strong deviation of the Tl electron cloud from the spherical form. This interaction, by means of directed *sp* and *p* orbitals, implies a partial charge transfer between Tl and Se atoms associated with a formation of Tl-Se-Tl chemical bonds. (Taking into account the coordination polyhedron around  $\text{Tl}^{1+}$ , one can speculate that *d* orbitals, perhaps in the form of *dsp* or *d^4sp*, are also included, yielding weak interaction with the neighbors. A contribution of *d* states of Tl into valence band of Tl selenides, sulphides, and tellurides was considered in Ref. 24).

A very surprising point is that  $\text{Tl}^{3+}$  ( $5d^{10}$ ) manifests a chemical shielding anisotropy that exceeds that of  $\text{Tl}^{1+}$  ( $5d^{10}6s^2$ ) by a factor of 4. It is clear that such a large shielding anisotropy may be caused only by the directed Tl-Se-Tl bonds in the (001) plane. As known, variation of the NMR chemical shift of a given element results from the paramagnetic contribution to chemical shielding  $\sigma_p$ . This term is due to the deviations from spherical symmetry of the electronic charge distribution. For an axially symmetric system,  $\sigma_p$  is not equal to zero only for nonzero angle  $\theta$  between  $B_0$  and bond direction<sup>25-27</sup> and usually shows  $\sigma_{\perp}$  in the high-frequency extreme and  $\sigma_{\parallel}$  in the low-frequency extreme.<sup>25,27</sup> However, one can see from Fig. 3 and Sec. V that the principal components of the chemical shielding tensor in TlSe are interchanged in comparison to this regular case. The chemical shift is maximal when the magnetic field is applied along the *c* axis. It means that the observed CSA cannot be described in terms of an intrachain cation-anion (Tl-Se) interactions only. The explanation of the opposite sign of CSA in TlSe requires including the overlap of the Tl-Se-Tl type in the (001) plane. We note that the similar effect is observed in aromatic systems such as benzene, hexafluorobenzene, etc., where the principal axis of the chemical shielding tensor (the most shielded direction) is

perpendicular to the molecular plane, and the least shielded direction is in the plane of ring carbons.<sup>28,29</sup>

We note that recent pseudopotential calculations of band structure and charge distribution in TlSe<sup>30</sup> showed that the uppermost valence bands and the first two conduction bands near the Tl(I) and Tl(III) atoms originate from *s* states of the Tl(I) and Tl(III) atoms, respectively (while four lowest valence bands are composed from the *s* states of Se). However, neither the interchain Tl(I)-Se-Tl(III) overlap nor the wavefunction delocalization within the valence and conduction band, observed in our experiments, were not reflected in the aforementioned calculation. One can conclude that further

theoretical work may yield new physical insights concerning band structure and charge distribution in TlSe.

In conclusion, we note that two-dimensional square lattice of TlSe in the (001) plane, with alternating univalent and trivalent ions, is not metallic at ambient temperature. However, significant overlap of electron wave functions in this plane allows us to expect an electron hopping between Tl<sup>1+</sup> and Tl<sup>3+</sup> ions at higher temperature, possibly accompanied by a phase transition into a metallic state. We note that high-pressure ambient temperature measurements of electrical resistivity of TlSe show that  $\rho_{\parallel}$  and  $\rho_{\perp}$  decrease continuously with pressure and reach metallic resistivities at  $P \sim 2.7$  GPa.<sup>31</sup>

\*Corresponding author. FAX: +972-8-6472-903. Email address: pan@bgumail.bgu.ac.il

<sup>1</sup>A. M. Panich, *Sov. Phys. Solid State* **31**, 1814 (1989).

<sup>2</sup>A. M. Panich, S. P. Gabuda, N. T. Mamedov, and S. N. Aliev, *Sov. Phys. Solid State* **29**, 2114 (1987).

<sup>3</sup>A. M. Panich and Th. Doert, *Solid State Commun.* **114**, 371 (2000).

<sup>4</sup>N. M. Gasanly, B. G. Akinoglu, S. Ellialtioglu, R. Laiho, and A. E. Bakhyshov, *Physica B* **192**, 371 (1993).

<sup>5</sup>J. A. Ketelaar, W. H. Hart, R. Moorel, and D. Polder, *Z. Kristallogr.* **101**, 396 (1939).

<sup>6</sup>S. Bradtmöller, R. K. Kremer, and P. Böttcher, *Z. Anorg. Allg. Chem.* **620**, 1073 (1994).

<sup>7</sup>E. Mooser and W. B. Pearson, *Phys. Rev.* **101**, 492 (1956).

<sup>8</sup>R. S. Itoga and C. R. Kannewurf, *J. Phys. Chem. Solids* **32**, 1099 (1971).

<sup>9</sup>S. Sugaike, *Mineral. J. Jpn.* **2**, 63 (1957).

<sup>10</sup>N. A. Abdullaev, M. A. Nizametdinova, A. D. Sadarly, and R. A. Suleymanov, *J. Phys.: Condens. Matter* **4**, 10 361 (1992).

<sup>11</sup>J. F. Hinton, K. R. Metz, and R. W. Briggs, in *Annual Reports of NMR Spectroscopy*, edited by G. A. Webb (Academic, London, 1982), Vol. 13, p. 211.

<sup>12</sup>J. H. Van Vleck, *Phys. Rev.* **74**, 1168 (1948).

<sup>13</sup>N. Bloembergen and T. J. Rowland, *Phys. Rev.* **97**, 1679 (1955).

<sup>14</sup>Y. Saito, *J. Phys. Soc. Jpn.* **21**, 1072 (1996).

<sup>15</sup>E. V. Kholopov, A. M. Panich, N. K. Moroz, and Yu. G. Kriger, *Zh. Eksp. Teor. Fiz.* **84**, 1091 (1983) [*Sov. Phys. JETP* **57**, 632 (1983)].

<sup>16</sup>A. Abragam, *The Principles of Nuclear Magnetism* (Clarendon, Oxford, 1961).

<sup>17</sup>J. W. Emsley, J. Feeney, and L. H. Sutcliffe, *High Resolution Nuclear Magnetic Resonance Spectroscopy* (Pergamon, New York, 1965), Vol. 1.

<sup>18</sup>J. A. Pople, W. G. Schneider, and H. J. Bernstein, *High-Resolution Nuclear Magnetic Resonance* (McGraw-Hill, New York, 1959).

<sup>19</sup>S. Meiboom, Z. Luz, and D. Gill, *J. Chem. Phys.* **27**, 1411 (1957).

<sup>20</sup>A. Carrington and A. D. McLachlan, *Introduction to Magnetic Resonance* (Harper & Row, New York, 1967).

<sup>21</sup>T. Shimizu, *J. Phys. Soc. Jpn.* **16**, 1264 (1961).

<sup>22</sup>H. A. Kramers, *Physica (Amsterdam)* **1**, 184 (1934).

<sup>23</sup>L. E. Orgel, *J. Chem. Soc.* **4**, 3815 (1959).

<sup>24</sup>L. Porte and A. Tranquard, *J. Solid State Chem.* **35**, 59 (1980).

<sup>25</sup>C. P. Slichter, *Principles of Magnetic Resonance* (Springer, Berlin, 1978).

<sup>26</sup>L. Landau and E. Lifshitz, *Quantum Mechanics* (Fizmatgiz, Moscow, 1963).

<sup>27</sup>A. M. Panich, *Synth. Met.* **100**, 169 (1999).

<sup>28</sup>M. Mehring, R. G. Griffin, and J. S. Waugh, *J. Chem. Phys.* **55**, 746 (1971).

<sup>29</sup>A. Pines, M. G. Gibby, and J. S. Waugh, *Chem. Phys. Lett.* **15**, 373 (1972).

<sup>30</sup>G. S. Orudzhev, Sh. M. Efendiev, and Z. A. Dzhakhangirov, *Fiz. Tverd. Tela (Leningrad)* **37**, 284 (1985) [*Sov. Phys. Solid State* **37**, 152 (1995)].

<sup>31</sup>M. K. Rabinal, S. Asokan, M. O. Godazaev, N. T. Mamedov, and E. S. R. Gopal, *Phys. Status Solidi B* **167**, K97 (1991).